Luminescence properties of composite nanofibers with different diameters prepared by electrospinning technology

H. YU[a*], Y. LI[a], Y. WU[a], Y. SHEN[a], B. CHEN[b]

[a]*College of Environmental and Chemical Engineering, Dalian Jiaotong University, Dalian, Liaoning 116028, P.R. China*

[b]*Department of Physics, Dalian Maritime University, Dalian, Liaoning 116026, P.R. China*

Various composite nanofibers composed of polystyrene (PS, $M_w \approx 98\,000$) and europium complex $Eu(DBM)_3phen$ (DBM is dibenzoylmethane; phen is 1,10-phenanthroline) were prepared by electrospinning technology. The mass ratio of $Eu(DBM)_3phen$ complex to PS was fixed to 1:100 in all composite fibers samples. Scanning electron microscopy (SEM) analysis indicated that the diameter size of the composite nanofibers could be adjusted in the range of 300-1000 nm by changing PS concentration, and their length remain the same of several tens centimeter. The luminescent properties of the composite nanofibers with different diameters were studied carefully in comparison to the pure $Eu(DBM)_3phen$ complex. The results showed that the luminescent decay time constant for the $^5D_0$-$^7F_2$ transitions in the composite fibers increased gradually with fibers diameter increase and became longer compared to that in the pure europium complex. Moreover these composite nanofibers exhibited the much better photostability than that of the pure complex, and the improvement degree of the photostability was closely related to the diameter size of the nanofibers. The novel luminescent composite nanofibers prepared in this work are expected to have potential applications in a wide variety of new technologies including the fields of material, energy and environment and so on.

(Received October 9, 2014; accepted March 19, 2015)

Keywords: Electrospinning nanofibers; Diameter; Luminescent properties.

1. Introduction

The luminescence properties of rare earth (RE) complexes have gained much scientific attention because of the antenna effect of ligands and the *f-f* electron transition of RE^{3+} ions, which promise their wide applications in laser, phosphor, and optical data storage devices [1-3]. However, the application of pure RE complexes is restricted due to their low processing ability, poor thermal stability, and low photostability. An acceptable way to overcome the impasse is to disperse RE complexes into inorganic[4], or organic/inorganic hybrid matrixes.[5]The polymer-capped RE complexes possess also were improved photoluminescence properties ,thermal stability and mechanically flexible.[6-8] The RE complexes incorporated into the polymer matrixes reflect a new type of materials with the characteristics of both the complexes and the matrix materials, making them applicable in a broad range of technology fields.

Synthesis of functionalized materials using a structuring process at the submicrometer – scale - nanotechnology is an international hot research field of fundamental and applied sciences. [9-12] A lot of chemical and physical methods have been used to prepare nanostructural materials with different morphologies such as fibers, wires, rods, belts and tubes and so on. [13,14] Among these ways electrospinning is one of the facile, versatile and useful technique for fabricating nanofibers which are exceptionally long in length and uniform in diameter. [15-17] The diameters of electrospinning fibers could range from tens of nanometers to several micrometers, and their morphology depends on the properties of solvent and the solution, as well as other processing variables.[18] By electrostatic spinning, various lanthanide oxide and composite nanowires of organic-RE complex compounds were recently successfully synthesized [19-23] and the photoluminescence properties of some prepared nanowires exhibit obviously variation compared with the bulk materials or the pure complex. [24,25] Zhang et al. reported that the photoluminescence stability of the composite fibers was considerably improved over the pure complex and the change of luminescence properties was determined by the mass ratios of rare-earth complex to polymers in the composite fibers of rare-earth complex and polymer by electrospinning.[26] Nevertheless, as for the composite fibers with fixed mass ratios of rare-earth complex to polymer, the effect of the fiber diameter on the luminescence properties was not reported.

In this paper, various $Eu(DBM)_3phen$/PS composite

fibers with intense brightness were prepared via electrospinning process (DBM is dibenzoylmethane, phen is 1,10-phenanthroline and PS is polystyrene). The mass ratio of $Eu(DBM)_3phen$ complex to PS was fixed to 1:100 in all composite fibers samples. Their diameters could be adjusted in the range of 300-1000 nm. Luminescence properties of the composite fibers were studied in comparison to that of the relevant pure europium complex. It is interesting to observe that the room temperature fluorescence lifetime for the $^5D_0$ level in the composite fibers considerably became longer compared to that in the pure europium complex and was increased gradually with the diameter of the composite fibers. The photoluminescence stability of the composite fibers is also improved over those of the pure europium complex.

2. Experimental

2.1 Sample preparation

Europium complex ($Eu(DBM)_3phen$) was synthesized according to the reported method in literature [27, 28] and the PS was synthesized using an emulsifier-free emulsion polymerization method.[29] A typical progress, an appropriate amount prepared PS was dissolved in 10 ml N, N-dimethylformamide (DMF) solution. Then, an appropriate amount of $Eu(DBM)_3phen$ was dissolved into the prepared different PS solutions, respectively. These solutions were stirred in order to be uniform. These final solutions were electrospun to produce composite fibers of $Eu(DBM)_3phen$ complex and PS. The mass ratio of $Eu(DBM)_3phen$ complex to PS was 1:100 in all electrospun solutions. The concentrations of the PS in final electrospun solutions were 7.5, 10 and 15% w/w, respectively. The $Eu(DBM)_3phen$/PS composite fibers, which were electrospun from 7.5, 10.0 and 15.0 wt % of PS solutions, were labeled as Eu/PS-1, Eu/PS-2 and Eu/PS-3 in the following, respectively (see Table 1). The schematic diagram of the electrospinning setup was shown in Fig. 1, which consisted of three major parts: a high-voltage power supply, a spinneret (a plastic needle) and a rotating collector drum. In the present electrospinning experiment, the applied voltage was 10.0 kV and the collection distance was 20 cm.

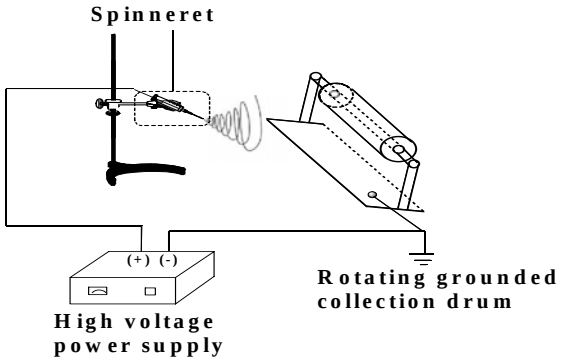

H. Q. Yu et al.

Fig. 1 Schematic diagram of the electrospinning setup.

Table 1. Composition of electrospinning solution

Sample	Concentration of Eu complex or PS in electrospinning solution		Ratio of Eu complex to PS in $Eu(DBM)_3phen$/PS composite fibers (w/w)
	Concentration of Eu complex in DMF solution	Concentration of PS in DMF solution	
Eu/PS-1	0.075 wt.%	7.5 wt.%	1 : 100
Eu/PS-2	0.01 wt.%	10.0 wt.%	1 : 100
Eu/PS-3	0.15 wt.%	15.0 wt.%	1 : 100

2.2 Measurements

The molecular weight (M_w) of PS powder was determined from high temperature gel permeation chromatography (GPC). A PL-GPC 220 chromatography system (Polymer Laboratories Ltd.) is composed of an online PD2040/DLS laser light scattering detector (Precision Detectors Inc.) and three PLgel 13 μm Olexis columns (300×7.5 mm). The eluent contained 1,2,4-trichlorobenzene (TCB, Acros) stabilized with 2,6-di-tert-butyl-4-methylphenol (5×10^{-4} g/mL, BHT, Acros) and was used after membrane (a pore size of 0.2 μm) filtration. The injection volume of the eluent was 200 μL, the flow rate was 1.0 mL/min and all measurements were performed at 150 °C. The morphology of the composite fibers was characterized with a Hitachi JSM-6360 scanning electron microscope. Fourier transform infrared spectra (FT-IR) were recorded in the range 4000-450cm^{-1} on a TENSOR 27. The excitation, emission spectra and fluorescence dynamics were obtained with a Hitachi F-4600 spectrophotometer using continuous 150 W Xe arc lamp radiation at room temperature. In order to compare various samples, the emission spectra were recorded at a fixed channel of 0.2 nm under the same conditions (PMT voltage, 400 V; both excitation and

emission split, 2.5 nm). In the process of determining the UV-induced spectral of the samples, the UV monochromic light was also irradiated from the same Xe arc lamp by monochromator at a slit of 10 nm.

3. Results and discussion

Fig. 2 is the GPC curve of the PS powder, showing that the PS had a molecular weight of 9.8×10^4 and a polydispersity index (M_W/Mn) of 2.65. Scanning electron microscopy (SEM) images of the composite fibers in different $Eu(DBM)_3Phen$/PS are shown in Fig. 3. It can be seen that the composite fibers had randomly oriented structures in the form of nonwoven mat, and the average diameters of composite fibers are about 300 nm (Fig. 3a), 500 nm (Fig. 3b) and 900 nm (Figure 3c) for Eu/PS-1, Eu/PS-2 and Eu/PS-3, respectively. It can be found that sample Eu/PS-2 exhibits uniform and superlong nanofibers, as shown in Figure 3d. Obviously, the diameters of the composite fibers increase as PS concentrations increase, but they remain the same length of several tens centimeter.

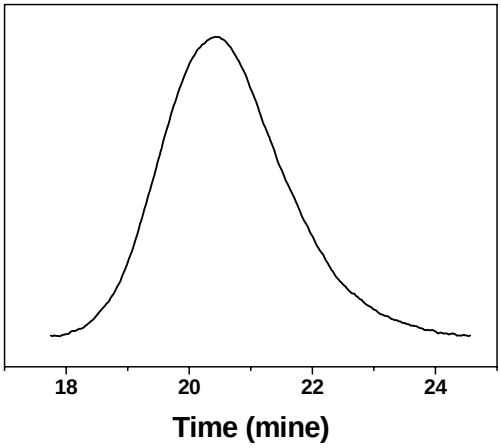

Fig. 2 GPC curve of PS powder at 150 °C.

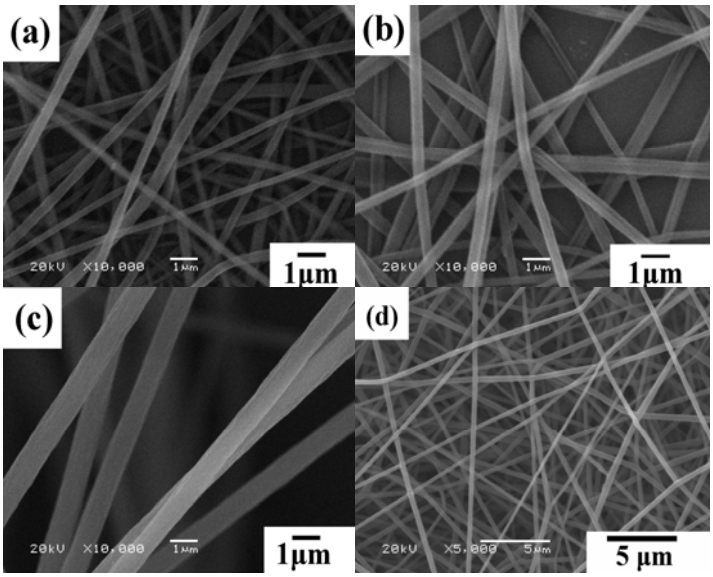

Fig. 3 SEM images of $Eu(DBM)_3Phen$/PS composition fibers: (a) Eu/PS-1, (b) Eu/PS-2, and (c) Eu/PS-3. (d) Image for sample Eu/PS-2 in a large scale.

Fourier transform infrared (FTIR) spectra of different samples are shown in Figure 4. The absorption bands of PS at 697, 756, 1028, 1450, 1492, and 1600 cm^{-1} are assigned to the vibration of the benzenoid ring [7, 30] and the broad band at 3400 cm^{-1} is attributed to the vibration of its associated hydroxyl groups. The peaks of Eu complex at around 1595 and 1517 cm^{-1} corresponds to the C=O stretching vibrations of DBM [31] and the peak centered at 1410 cm^{-1} corresponds to asymmetric stretching vibration of C=N in 1,10-phenanthroline.[32]

The weak peak at 464 cm^{-1} could be attributed to the Eu-O stretching vibration.[8, 33] It can be found that $Eu(DBM)_3$phen/PS composite fibers have the similar characteristic IR peaks as the pure PS, but the characteristic peaks of $Eu(DBM)_3$phen are not present in the corresponding range, this is perhaps that the vibration of ligands in $Eu(DBM)_3$phen be hided by the surrounding PS matrix. [26]

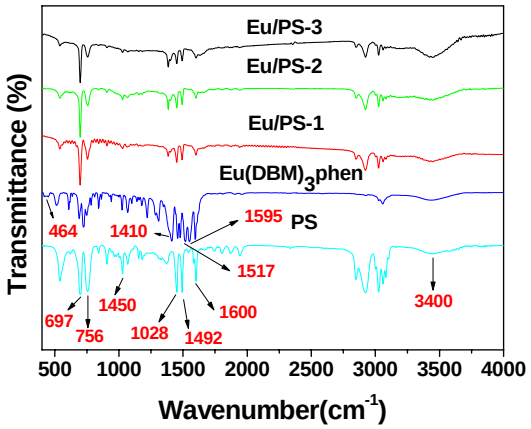

Fig. 4 FTIR spectra of the pure Eu(DBM)$_3$phen complex, pure PS, and Eu(DBM)$_3$phen/PS composite fibers (samples Eu/PS-1, Eu/PS-2 and Eu/PS-3).

Fig. 5 shows excitation and emission spectra of various samples. As for pure Eu(DBM)$_3$phen, there is a broad excitation band from 200 to 500 nm (inset of Fig. 5a), which is due to the π-π* electron transition of ligands. In the composite fibers, interestingly, the excitation band split into two peaks at ~ 280 and ~ 370 nm (Fig. 5a), respectively. This indicates that the site symmetry may become lower in the composite fibers due to the existence of the surrounding PS. [26] In addition, there is a $^7F_0$-$^5D_2$ excitation line in the excitation spectrum of pure Eu(DBM)$_3$phen, while the lines disappear in the spectrum of composite fibers. This suggests that the *f-f* inner-shell transitions in the composite fibers may be quenched through the nonradiative energy transfer from the higher excited states to some uncertain defect levels, which substitutes the nonradiative relaxation from higher excited states to $^5D_0$. In the emission spectra shown in Fig. 5b, the green emissions of $^5D_1$-$^7F_1$ below 550 nm are absent, while the red $^5D_0$-^7F_J (J = 0, 1, 2, 3, 4) transitions are observed. Among these lines, the $^5D_0$-$^7F_2$ line at 612 nm is dominant compared to any other line, and the peak locations, the intensity ratio of $^5D_0$-$^7F_1$ to $^5D_0$-$^7F_2$ are almost unchanged in different samples. From Fig. 5c, it can be found that the luminescent intensity of Eu(DBM)$_3$phen/PS composite fibers increases gradually with fibers diameter increase, although the ratio of Eu complex relative to PS in different samples remains the same.

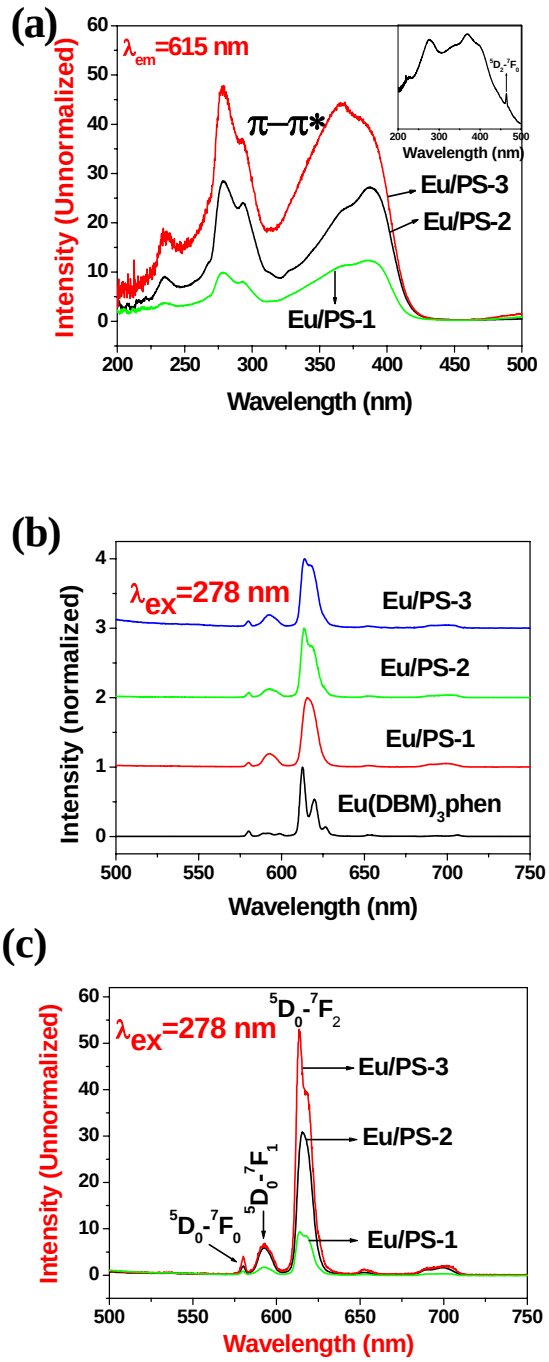

Fig. 5 (a) Excitation spectra of pure Eu(DBM)$_3$phen complex (Inset) and the Eu(DBM)$_3$phen/PS composite fibers (λ_{em}=615 nm). (b) Normalized and (c) Unnormalized emission spectra of the Eu(DBM)$_3$phen/PS composite fibers under 278 nm excitation.

The fluorescence decay curves of $^5D_0$-$^7F_2$ emissions for Eu^{3+} with the 254 nm excitation light were measured at room temperature, as shown in Fig. 6. It can be seen that the fluorescence decays exponentially for all the samples and the exponential lifetimes for $^5D_0$ states are obtained as 390, 810, 890 and 950 μs in pure $Eu(DBM)_3phen$, Eu/PS-1, Eu/PS-2 and Eu/PS-3, respectively. It can be easily proved that the fluorescence lifetime for the $^5D_0$ state in the composite fibers becomes longer compared to that in the pure europium complex and increases gradually with an increase in diameter of $Eu(DBM)_3phen$/PS composite fibers.

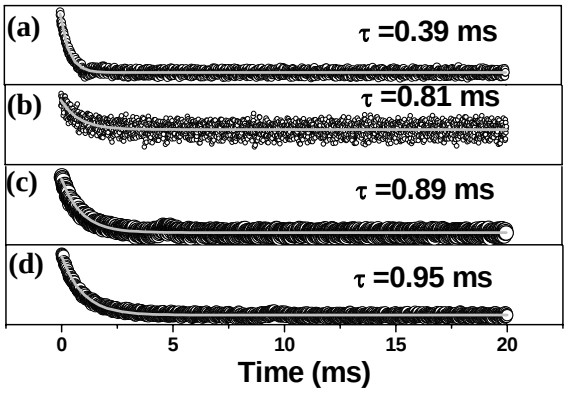

Fig. 6 Decay curves of various samples. (a), (b), (c) and (d) are corresponding to pure Eu(DBM)$_3$phen complex, Eu/PS-1, Eu/PS-2 and Eu/PS-3, respectively. The black circles are experimental data, and the grey solid lines are fitting functions.

The photoluminescence stability in different samples were also studied by comparing ultraviolet light irradiation-induced spectral changes. Fig. 7 shows the dependence of normalized emission intensity at 612 nm on irradiation time of the different samples, and it exhibits that the emission intensity of the $^5D_0$-$^7F_2$ transition in the pure $Eu(DBM)_3phen$ complex decreases with longer exposure time, whereas the emission intensity keeps nearly constant in sample Eu/PS-1. It is more interesting to find that the fluorescence intensity even increases with increasing exposure time in samples Eu/PS-2 and Eu/PS-3. In fact, the PS polymer provides a rigid environment for the pure complex to reduce the energy consumption of vibrations of ligands and intermolecular collisions of complexes, so the rigid PS molecule protects the pure complexes from decomposing under UV irradiation. The intensity enhancement with exposure time in the composite fibers can be attributed to optical modification of the surface defects that are involved between the pure complex and PS during the preparation of this material. Under UV exposure, the surface defects acted as nonradiative relaxation channels are gradually modified, causing the photoluminescence to increase.

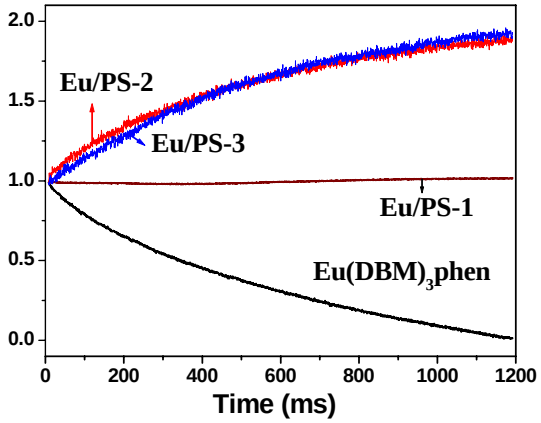

Fig. 7 Dependence of normalized intensity at 609 nm on irradiation time in different samples. The samples are irradiated by 278-nm light.

4. Conclusions

In summary, uniform $Eu(DBM)_3phen$/PS composite fibers were prepared successfully by electrospinning process and their photoluminescence properties were studied in comparison to that of the pure complex. The results demonstrate that the excitation bands of the π-π* electron transition of the ligands split into different components because of the distortion of the crystal field. The fluorescence lifetimes of the Eu^{3+} $^5D_0$-$^7F_2$ transitions in the composite fibers considerably became longer compared to that in the pure europium complex, and they increased gradually with an increase of the fiber diameter of $Eu(DBM)_3phen$/PS composite. Most of all, the fluorescence emission intensity of composite fibers increased with increasing exposure time under UV irradiation owing to the modified polymer matrixes. The photostability of the luminescence for the composite fibers improved considerably in comparison to that for the $Eu(DBM)_3phen$ complex. The novel luminescent composite fibers prepared in this work are expected to have potential applications in a wide variety of new technologies.

Acknowledgments

The authors thank the financial supports from the National Natural Science Foundation of China (Grant No. 50802010, 50972021, 21076028 and 61078061), the Program for Liaoning Excellent Talents in University

(Grant No. LJQ2011047) and the Program for Liaoning BaiQianWan Talents (Grant No. 2014921063).

Reference

[1] C. Yan, C. Guo, P. Lu, M. Zhang, G. Qiu, J. Rare. Earth. **25**, 117 (2007)
[2] Y. Zhang, Y. Zhou, G. Accorsi, N. Armaroli, J. Rare. Earth. **26**, 173 (2008)
[3] Q. Xu, L. Li, X. Liu, R. Xu, Chem. Mater. **14**, 549 (2002)
[4] A. Fernandes, J. Dexpert-Ghys, A. Gleizes, A. Galarneau, D. Brunel, Microporous Mesoporous Mater. **83**, 35 (2005)
[5] L. R. Matthews, E. T. Knobbe, Chem. Mater. **5**, 1697 (1993)
[6] H. Zhang, H. Song, H. Yu, S. Li, X. Bai, G. Pan, Appl. Phys. Lett. **90**, 103103 (2007)
[7] H. Zhang, H. Song, B. Dong, L. Han, G. Pan, X. Bai, L. Fan, S. Lu, H. F. Zhao, F. Wang, J. Phys. Chem. C. **112,** 9155 (2008)
[8] X. Zhang, S. Weng, S. Hu, L. Zhang, L. Liu, J. Rare. Earths. **28**, 333 (2010)
[9] Y. Xia, P. Yang, Y. Sum, Y. Wu, B. Mayers, B. Gates, Y. Yin, F. Kim, H. Yan, Adv. Mater. **15**, 353 (2003)
[10] D. Younesi, R. Mehravaran, S. Akbarian, M. Younesi, Mater. Des. **43**, 549 (2013)
[11] C. Zhao, B. P. Zhang, S. J. Wang, P. P. Shang, S. Li, L. P. Yan, Mater. Des. **32**, 947 (2013)
[12] N. Nouri, S. Ziaei-Rad, S. Adibi, F. Karimzadeh, Mater. Des. **34**, 1 (2012)
[13] Y. Xia, P. Yang, Adv. Mater. **15**, 351 (2003)
[14] K. Ariga, M. Li, G. J. Richards, J. P. Hill, J. Nanosci. Nanotechnol. **11**, 1 (2011)
[15] R. P. Kumar, N. Khan, S. Vivekanandhan, N. Satyanarayana, A. K. Mohanty, M. Misra, J. Nanosci. Nanotechnol. **12**, 1 (2012)
[16] W. D. Shi, S. Y. Song and H. J. Zhang, Chem. Soc. Rev. **42,** 5714 (2013).
[17] S. L. Sampson, L. Saraiva, K. Gustafsson, S. N. Jayasinghe, B. D. Robertson, Small. **10,** 78 (2014).
[18] R. Masoodi, R. F. El-Hajjar, K. M. Pillai, R. Sabo, Mater. Des. **36**, 570 (2012)
[19] Z. Hou, G. Li, H. Lian, J. Lin, J. Mater. Chem. **22**, 5254 (2012)
[20] C. Y. Xu, J. Z. Guo, Y. D. Li, H. J. Seo, Opt. Mater. **35**, 893 (2013).
[21] L.Y. Yang, J. X. Wang, X. T. Dong, G. X. Liu, W. S. Yu, J. Mater. Sci. **48,** 644 (2013).
[22] Z. Y. Hou, X. J. Li, C. X. Li, Y. L. Dai, P. A. Ma, X. Zhang, X. J. Kang, Z. Y. Cheng, J. Lin, Langmuir **29,** 9473 (2013).
[23] M. Liu, H. Liu, S. F. Sun, X. J. Li, Y. M. Zhou, Z. Y. Hou, J. Lin, Langmuir **30,** 1176 (2014).
[24] H. Song, H. Yu, G. Pan, X. Bai, B. Dong. X. T. Zhang, S. K. Hark, Chem. Mater. **20**, 4762 (2008)
[25] L. Xu, H. Song, B. Dong, Y. Wang, X. Bai, G. Wang, Q. Liu, J. Phys. Chem. C **11**3 , 9609 (2009)
[26] H. Zhang, H. Song, H. Yu, X. Bai, S. Li, G. Pan, Q. Dai, T. Wang, W. Li, S. Lu, X. Ren, H. Zhao, J. Phys. Chem. C **111**, 6524 (2007)
[27] L. R. Melby, N. J. Rose, E. Abramson, J. C. Caris, J. Am. Chem. Soc. **86**, 5117 (1964)
[28] P. S. Chowdhury, S. Saha, A. Patra, Chem. Phys. Lett. **405,** 393 (2005)
[29] B. T. Holland, C. F. Blanford, T. Do, A. Stein, Chem. Mater. **11**, 795 (1999)
[30] D. W. Dong, S. Tasaka, N. Inagaki, Polym. Degred. Stabil. **72**, 345 (2001)
[31] C. H. Yan, C. F. Guo, P. Lu, M. Zhang, G. M. Qiu, J. Rare. Earth. **25**, 117 (2007)
[32] Y. G. Lv, J. Y. Zhang, W. L. Cao, F. J. Zhang, Z. Xu, J. Rare. Earth. **25,** 296 (2007)
[33] N. C. Chang, J. B. Gruber, J. Chem. Phys. **41,** 3227 (1964)

*Corresponding author: yuhq7808@djtu.edu.cn